Lifetime Persistence and Clonality of Chromosome Aberrations in the Peripheral Blood of Mice Acutely Exposed to Ionizing Radiation

Authors: Michelle D. Spruill, David O. Nelson, Marilyn J. Ramsey, Joginder Nath, and James D. Tucker

Source: Radiation Research, 153(1) : 110-121

Published By: Radiation Research Society

URL: https://doi.org/10.1667/0033-7587(2000)153[0110:LPACOC]2.0.CO;2

RADIATION RESEARCH **153**, 110–121 (2000)
0033-7587/00 $5.00

Lifetime Persistence and Clonality of Chromosome Aberrations in the Peripheral Blood of Mice Acutely Exposed to Ionizing Radiation

Michelle D. Spruill,[a] David O. Nelson,[b] Marilyn J. Ramsey,[b] Joginder Nath[c] and James D. Tucker[b,1]

[a]*Toxicology and Molecular Biology Branch, MS 3014, National Institute for Occupational Safety and Health, 1095 Willowdale Road, Morgantown, West Virginia 26505;* [b]*Biology and Biotechnology Research Program, L-452, P.O. Box 808, Lawrence Livermore National Laboratory, Livermore, California 94551; and* [c]*Genetics and Developmental Biology Program, College of Agriculture and Forestry, P.O. Box 6108, West Virginia University, Morgantown, West Virginia 26505*

Spruill, M. D., Nelson, D. O., Ramsey, M. J., Nath, J. and Tucker, J. D. Lifetime Persistence and Clonality of Chromosome Aberrations in the Peripheral Blood of Mice Acutely Exposed to Ionizing Radiation. *Radiat. Res.* 153, 110–121 (2000).

As the measurement of chromosomal translocations increases in popularity for quantifying prior radiation exposure, information on the possible decline of these ''stable'' aberrations over time is urgently needed. We report here information about the persistence of radiation-induced chromosome aberrations *in vivo* over the life span of a rodent. Female C57BL/6 mice were given a single whole-body acute exposure of 0, 1, 2, 3 or 4 Gy ^{137}Cs γ rays at 8 weeks of age. Chromosome aberrations were analyzed from peripheral blood samples at various intervals between 1 day and 21 months after exposure. Aberrations were detected by painting chromosomes 2 and 8. Translocations decreased dramatically during the first 3 months after irradiation, beyond which time the frequencies remained relatively constant out to 1 year, when the effects of aging and clonal expansion became significant. Both reciprocal and nonreciprocal translocations increased with age in the unexposed control animals and were involved in clones. As expected of unstable aberrations, dicentrics decreased rapidly after exposure and reached baseline levels within 3 months. These results indicate that the persistence of translocations induced by ionizing radiation is complicated by aging and clonal expansion and that these factors must be considered when quantifying translocations at long times after exposure. These results have implications for biological dosimetry in human populations.

INTRODUCTION

The Radiation Effects Research Foundation has analyzed data from 1703 atomic bomb survivors from Hiroshima and Nagasaki in an attempt to derive the doses of radiation to which these people were exposed (*1*). The success of this endeavor and others attempting to estimate doses from incidents where many years have passed since exposure, such as the Chernobyl nuclear reactor accident (*2*), is dependent on knowledge concerning the persistence of translocations over time.

Until recently, there was little information on the possible decline of stable aberrations over time. Fluorescence *in situ* hybridization with whole-chromosome probes, ''chromosome painting'', has increased the ease, speed and sensitivity with which translocations can be detected in human cells (*2–9*) and has led to the use of animal models (*10–17*) to evaluate this question, which could not have been approached previously.

The present work was designed to assess the stability of radiation-induced chromosome aberrations *in vivo* over the life span of a rodent, and it extends the results of our previous publication (*16*) in which we examined the persistence of aberrations for 1 month after acute exposure. After whole-body exposure to 0, 1, 2, 3 or 4 Gy ^{137}Cs γ rays, the persistence of reciprocal translocations, nonreciprocal translocations and dicentrics was measured in peripheral blood lymphocytes. Reciprocal translocations and dicentrics are both two-lesion events that are theorized to be induced at equal frequencies (*18*). They are both characterized by two color junctions in painted cells. However, a reciprocal translocation is a symmetrical interchange that is thought to be stable because each resulting chromosome has only one centromere and there is no visible loss of genetic material. A dicentric, on the other hand, is an asymmetrical exchange resulting in one chromosome with two centromeres and an acentric fragment that lacks a centromere altogether. Cells with dicentrics are known to be eliminated during cell division. Nonreciprocal translocations, in contrast to reciprocal translocations, appear as only one color junction in painted cells. While some nonreciprocal translocations may actually be reciprocal events in which one color junction is too small to be visualized, our previous publication (*16*) showed the difference in their persistence in rapidly dividing bone marrow cells, suggesting that they are a separate class of aberrations, possibly arising from the resolution of chromatid exchanges (quadriradials). We found a significant decrease in translocations during the first 3 months

[1] Author to whom correspondence should be addressed.

after irradiation, beyond which time the frequency remained relatively constant. Both reciprocal and nonreciprocal translocations were found to increase with age in the unexposed control animals. As expected, dicentrics decreased rapidly after exposure and did not increase with age in controls. Clonal expansion of cells bearing reciprocal as well as nonreciprocal translocations was found to be a confounding factor that contributed significantly to the variation among exposed as well as unexposed mice. The findings of this study illustrate several difficulties associated with performing biological dosimetry at long times after exposure, and these may have an impact on retrospective dose estimation in humans.

MATERIALS AND METHODS

Animals and Radiation Exposure

Female C57BL/6 mice were received from Simonson (Gilroy, CA) and Jackson Laboratory (Bar Harbor, ME) approximately 7 weeks after birth and were quarantined for 1 week prior to exposure. The animals were housed under conditions of controlled temperature (72°F) and humidity (45%) and a 12-h light/dark cycle. Animals were fed pelleted Purina rodent chow and given sterile drinking water *ad libitum.* At 8 weeks of age, the mice were given a single acute dose of 0, 1, 2, 3 or 4 Gy ^{137}Cs γ rays at a dose rate of approximately 80 cGy/min. The mice were placed on a rotating turntable to ensure an even, whole-body exposure. The animal experiments were approved by the Institutional Animal Care and Use Committee of Lawrence Livermore National Laboratory.

Tissue Isolation, Cell Culture and Slide Preparation

Peripheral blood was isolated from four anesthetized mice in each dose group at 1, 8, 15 and 30 days, 2 months, 3 months, and every 3 months thereafter until 21 months postirradiation. The peripheral blood was isolated by cardiac puncture and cultured for 36 h as described previously (*16*) using 60 μg/ml lipopolysaccharide as a mitogen. Colcemid (0.1 μg/ml) was added for the last 12 h of culture to collect metaphase cells. Metaphase chromosome spreads were prepared according to standard protocols.

In animals exposed to 4 Gy, we were unable to obtain a sufficient number of metaphase cells 1 day after exposure. Two repeated attempts using different animals were unsuccessful in obtaining usable cells. This was presumably due to radiation toxicity, manifested as severe cell cycle delay.

Fluorescence In Situ Hybridization

Chromosome painting was performed as described previously (*16*) using biotinylated whole-chromosome probes specific for chromosomes 2 and 8. Microscope slides with chromosomal material that proved difficult to hybridize were sometimes soaked in either 0.5% Tween 20 in PBS for 5 min or 0.2 *M* HCl for 20 min prior to denaturation. Cells were counterstained with propidium iodide and 4′-6-diamidino-2-phenylindole (DAPI).

Microscopy and Scoring of Aberration

Zeiss Axioskop or Axiophot fluorescence microscopes equipped with wide band-pass filters were used to visualize fluorescein-labeled chromosomes counterstained with propidium iodide. A DAPI filter was used to visualize centromere staining. Aberrations were scored by a single observer and categorized using the PAINT system (*8*). All slides were coded prior to scoring to minimize observer bias. Metaphase cells were scored only if they met the following criteria: (1) The cells were well spread and the hybridization signal was sufficient to detect exchanges; (2) the centromeres of all chromosomes were readily identifiable under DAPI illumination; and (3) the cells appeared complete and contained the centromeres derived from the four painted chromosomes. Photographs were taken of all abnormal cells. This allowed us to store complete information about each chromosome aberration for later analysis. Only those aberrations involving painted chromosomes were counted in the results.

Mouse chromosomes 2 and 8 together comprise 11.5% of the genome (*19*); therefore, we detected approximately 20.5% of all simple interchanges (*17*), and approximately five painted metaphase cells yielded the same amount of information as one G-banded cell. One hundred cell equivalents (approximately 500 actual metaphase cells) were scored from each tissue for each mouse where available.

Analysis of Clones

Clones were identified by comparing the color photographs of all cells containing stable aberrations. Determination of clonality was made on the basis of similar breakpoint locations or the presence of other identifying characteristics such as unusual aberrations. To correct the frequency of translocations for the presence of clones, each clone, regardless of how many cells it contained, was counted only once. This adjusted value reflects the original (i.e. induced) aberration frequency since each clone, by definition, originated as a single cell. Abnormal cells from every mouse aged 3 to 21 months after exposure were analyzed for clones. Prior to 3 months, clones were not apparent, so they did not contribute significantly to the translocation frequency.

Statistical Analysis

Estimating the equality of rates of translocations and dicentrics. The equality of the rates of translocations and dicentrics was evaluated by χ^2 tests. The null hypothesis was that, for a given combination of dose and aberration type (translocation or dicentric), the rate of translocations was equal to the rate of dicentrics; i.e., the ratio of the rates was one. The alternative hypothesis was that the ratio of the rate of translocations to that of dicentrics was constant, but not necessarily one. Chi-square tests were performed as described in ref. (*20*). Briefly, the χ^2 statistic for a test is formed by treating the predicted values under the alternative as ''observed'' and testing goodness of fit to the predicted values under the null. The degree of freedom for the test is 1, the difference between the number of parameters estimated under the null and the alternative. The number of predicted (or expected) events was computed as follows. For the hypothesis where the rate ratio is 1, the number of expected events for a given type of aberration, dose and outcome is just one-half of the total number of events for that given type of aberration and dose. For the hypothesis where the rate ratio is some unknown value other than 1, computing the expected number of events proceeds in two steps. First, the rate ratio between translocations and dicentrics is estimated by dividing the sum of translocation events ($n = 375$) by the sum of dicentric events ($n = 336$). Second, the expected number of events for each type of aberration, dose and outcome combination is calculated by requiring that (1) the total number of expected events for the type of aberration and dose is equal to the total number of observed events, and (2) the ratio of the two expected event counts is equal to the estimated rate ratio (approximately 1.116).

Overdispersion. For Poisson random variables with mean μ, the variance $V(\mu)$ is equal to μ. A random variable of counts is said to be overdispersed, or to exhibit *extra-Poisson variation,* when $V(\mu) > \mu$. For data in the form of counts, overdispersion is the norm rather than the exception. Failing to account for overdispersion will produce standard errors that are too small and *P* values that can be misleadingly ''significant.'' We performed tests for two common types of overdispersion:

$$V(\mu) = \mu\,(1 + c\mu) \text{ and } V(\mu) = \mu\,(1 + c),$$

for some unknown constant $c > 0$. The first test is sensitive to overdispersion where the variance increases roughly as the square of the mean,

TABLE 1
Observed and Predicted Numbers of Translocations and Dicentrics 1 Day after Exposure of Mice to Acute Whole-Body ^{137}Cs γ Radiation

	Observed events		Predicted events with a common rate ratio			
			Rate ratio = 1		Rate ratio ≠ 1	
	Translocations	Dicentrics	Translocations	Dicentrics	Translocations	Dicentrics
Nonreciprocal events (one color junction)						
1 Gy	9	5	7.0	7.0	6.3	7.7
2 Gy	9	13	11.0	11.0	9.9	12.1
3 Gy	26	23	24.5	24.5	22.1	26.9
Reciprocal events (two color junctions)						
1 Gy	14	15	14.5	14.5	13.1	15.9
2 Gy	22	24	23.0	23.0	20.7	25.3
3 Gy	42	69	55.5[a]	55.5[a]	50.0	61.0
Goodness of fit			$\chi^2 = 8.74$ (6 *df*) $P = 0.19$		$\chi^2 = 6.11$ (5 *df*) $P = 0.30$	

[a] Expected values correspond to cells which contributed 3 or more to χ^2 for goodness of fit.

while the second is sensitive to overdispersion where the variance increases in proportion to the mean. Estimating and accounting for nonlinear mean–variance relationships $V(\mu)$ is an ongoing area of statistical research. The first type of overdispersion is related to negative binomial models and is described in more detail in the Appendix. The second type of overdispersion is more heuristic. However, the constant c is easy to estimate, and hence it is often used as a scale factor to provide more realistic standard errors and P values for data which are ostensibly Poisson.

Estimating the background age effect. The background age effect was estimated for each outcome by a Poisson generalized linear model with an exponential age effect:

$$\log b(t) = a_0 + a_1 t,$$

where $b(t)$ is the average background outcome frequency at time t. The estimated background frequencies as a function of time were then used in subsequent exponential fits.

Fitting persistence curves. The persistence of translocations over time was analyzed by fitting exponential decay models to the data on translocations using S-PLUS (*21*). These models describe curves that start out at an initial high value and decay at some rate to a horizontal line (the asymptote) as time increases. Various models were fitted for each data set to determine if the initial values, decay rates, or asymptotes were the same for various doses. Comparisons between models were performed using likelihood ratio tests. See the Appendix for a more detailed description of the fitting procedures used.

RESULTS

Equality of Frequencies of Translocations and Dicentrics

Table 1 shows the results of testing whether or not translocations and dicentrics observed in the peripheral blood 1 day after exposure have a common rate, as a function of dose and number of junctions (i.e. reciprocal or nonreciprocal for translocations, and presence or absence of a bicolored fragment for dicentrics). The alternative hypothesis was that the two end points have a common rate ratio, but that this ratio may not be one. The χ^2 goodness of fit shows no significant deviation from Poisson for either hypothesis. Comparing the two models results in a χ^2 value of 2.69 on 1 degree of freedom ($P = 0.10$). Examination of Table 1 shows that the improvement in fit for the model where the rate ratio ≠ 1 is largely due to a better fit for cells with reciprocal exchanges exposed to 3 Gy. In any event, the improvement is not dramatic enough to produce a significant result.

Table 2 shows similar results for the data at 8 days after exposure. Here the comparison of the two models produces a χ^2 value of 2.14 on 1 degree of freedom ($P = 0.14$). However, both models produce goodness-of-fit results that indicate a poor fit to the assumptions of the model. The counts of translocations and dicentrics for 2 Gy are far apart, indicating that the rate ratio for 2 Gy may be different from the rate ratios for the other exposures. By 15 days after exposure, equality of the frequencies of translocations and dicentrics no longer existed (data not shown).

Overdispersion

In the subset of observations between days 8 and 365, we found some evidence suggesting overdispersion. For reciprocal translocations, the overdispersion was not enough to warrant using a negative binomial model ($P > 0.05$). There was significant evidence of overdispersion for nonreciprocal translocations ($P < 10^{-5}$), so a negative binomial model was employed for these data.

Background Age Effect

We observed an age effect in the unexposed (control) mice which was particularly noticeable after 1 year. Reciprocal and nonreciprocal translocations were both found to increase with age (Figs. 1 and 2, respectively). The fitted equation for reciprocal translocations was

$$b(t) = \exp(-8.07 + 1.85 \times \text{years}),$$

TABLE 2
Observed and Predicted Numbers of Translocations and Dicentrics 8 Days after Exposure of Mice to Acute Whole-Body ^{137}Cs γ Radiation

	Observed events		Predicted events with a common rate ratio			
			Rate ratio = 1		Rate ratio ≠ 1	
	Translocations	Dicentrics	Translocations	Dicentrics	Translocations	Dicentrics
Nonreciprocal events (one color junction)						
1 Gy	3	4	3.5	3.5	3.7	3.3
2 Gy	10	2	6.0	6.0	6.3	5.7
3 Gy	39	56	47.5	47.5	50.1	44.9
4 Gy	95	70	82.5	82.5	87.0	78.0
Reciprocal events (two color junctions)						
1 Gy	8	6	7	7	7.3	6.6
2 Gy	21	6	13.5[a]	13.5[a]	14.2[a]	12.8[a]
3 Gy	82	63	72.5	72.5	76.5	68.5
4 Gy	117	129	123.0	123.0	129.8	116.2
Goodness of fit			$\chi^2 = 24.00$ (8 *df*) $P = 0.0023$		$\chi^2 = 21.93$ (7 *df*) $P = 0.0026$	

[a] Expected values correspond to cells which contributed 3 or more to χ^2 for goodness of fit.

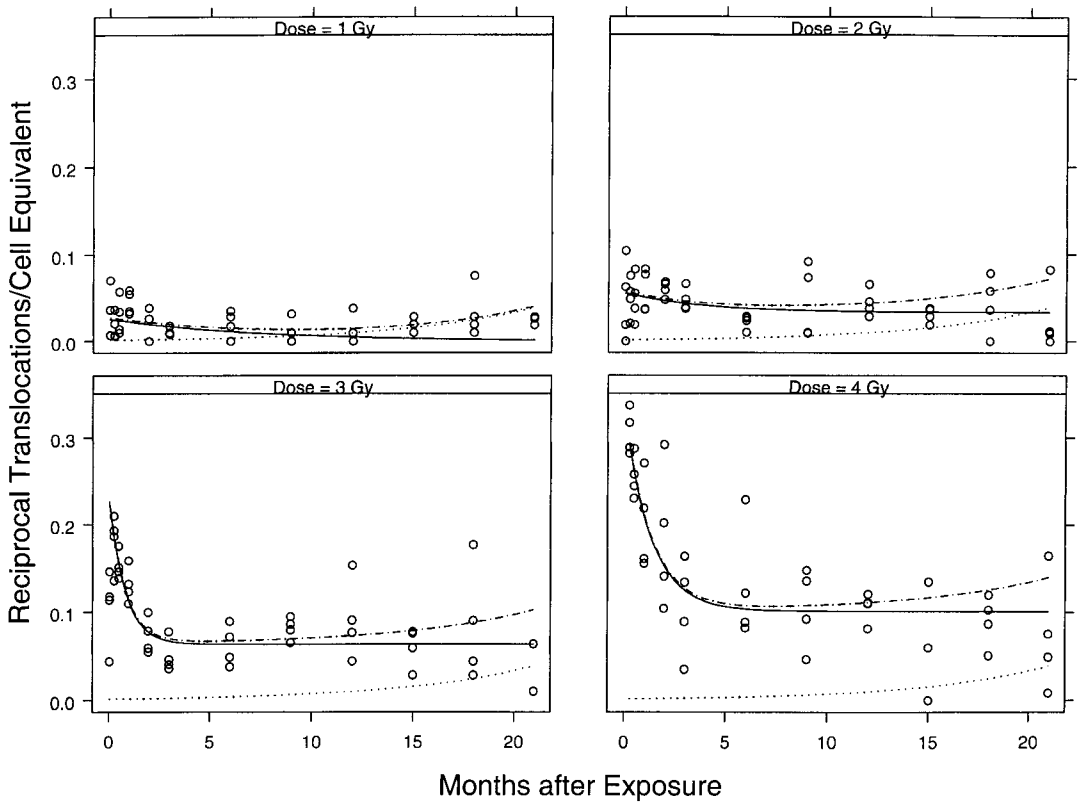

FIG. 1. Persistence of reciprocal translocations in the peripheral blood lymphocytes of mice exposed to 1, 2, 3 or 4 Gy ^{137}Cs γ rays. Solid lines are the weighted least-squares regression fits to the data from 8 days to 1 year, and projected to the end of the study (21 months). Dotted lines are the weighted least-squares regression fits to data from the unexposed mice from all sampling times (data points not shown for control animals). Dashed lines represent the sum of the solid and dotted lines.

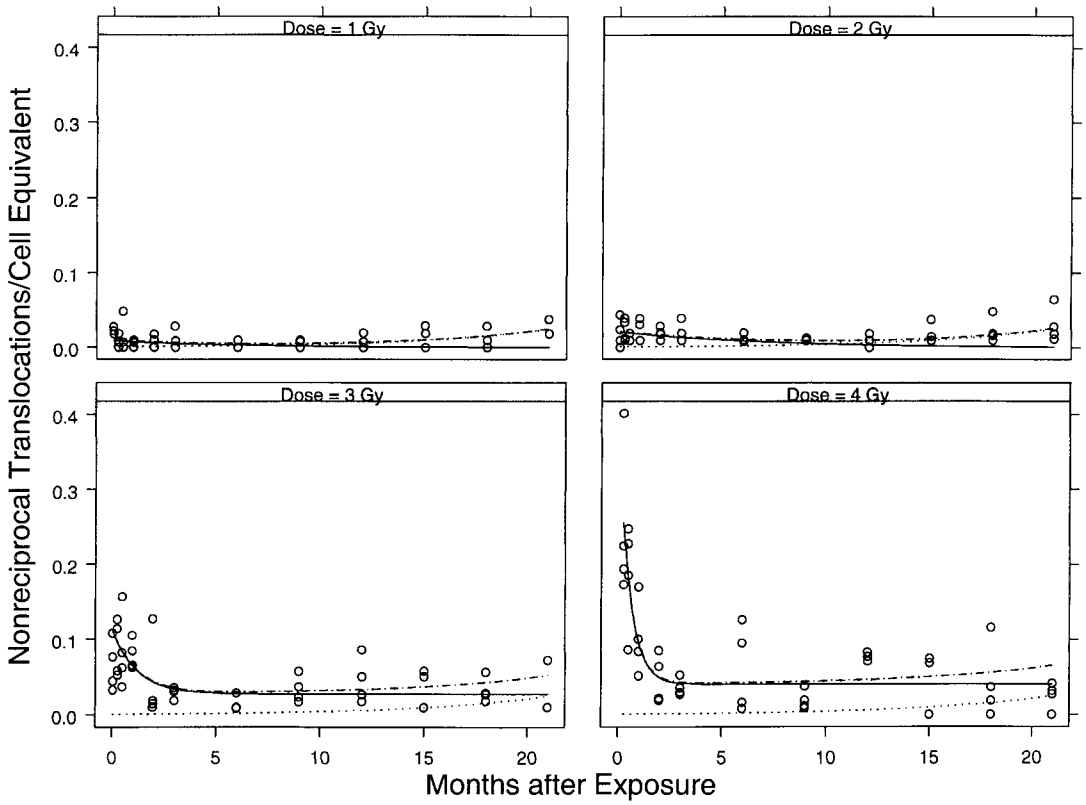

FIG. 2. Persistence of nonreciprocal translocations in the peripheral blood lymphocytes of mice exposed to 1, 2, 3 or 4 Gy ^{137}Cs γ rays. Solid lines are the weighted least-squares regression fits to the data from 8 days to 1 year, and projected to the end of the study (21 months). Dotted lines are the weighted least-squares regression fits to data from the unexposed mice from all sampling times (data points not shown for control animals). Dashed lines represent the sum of the solid and dotted lines.

TABLE 3
Coefficient Estimates and Standard Errors of the "Best" Exponential Fit to Reciprocal Translocation Data from Day 8 through Day 365

Coefficient	Value	SE	*P* value
A_i (Asymptote)			
1 Gy	0.0×10^{-3}	2.9×10^{-3}	1.00
2 Gy	6.8×10^{-3}	1.9×10^{-3}	4.10×10^{-4}
3 Gy	13.0×10^{-3}	1.3×10^{-3}	$<1.00 \times 10^{-10}$
4 Gy	20.7×10^{-3}	1.9×10^{-3}	$<1.00 \times 10^{-10}$
B_i (Initial)			
1 Gy	5.3×10^{-3}	2.9×10^{-3}	0.07
2 Gy	4.5×10^{-3}	2.3×10^{-3}	0.05
3 Gy	34.5×10^{-3}	6.6×10^{-3}	8.16×10^{-7}
4 Gy	47.8×10^{-3}	6.8×10^{-3}	1.29×10^{-10}
C_i (Decay)			
1 Gy	1.6	1.7	0.35
2 Gy	3.1	3.7	0.40
3 Gy	15.2	4.0	2.27×10^{-4}
4 Gy	9.2	2.4	2.50×10^{-4}

Notes. Model was of the form $A_i + B_i \exp(-C_i t)$, with all coefficients constrained to be non-negative. Errors were assumed to be Poisson. Only data from days 8 through 365 were used to estimate the coefficients. (See the Materials and Methods for details.)

while the fitted equation for nonreciprocal translocations was

$$b(t) = \exp(-8.63 + 1.91 \times \text{years}).$$

The coefficients for reciprocal and nonreciprocal translocations were not significantly different from each other. The size of the residual deviance when compared to the degrees of freedom indicates no appreciable overdispersion among unexposed mice, even at later ages. We have described elsewhere the age effect in these and other unexposed mice from our laboratory (*22*).

Persistence of Translocations

Tables 3 and 4 show the coefficients, standard errors, and asymptotic *P* values for the best-fitting exponential decay models for reciprocal and nonreciprocal translocations, respectively. As explained in the Materials and Methods, three increasingly less restricted models were fitted to the data for dose >0 and days 8 through 365. A likelihood ratio test comparing the three models indicated a significantly better fit with each more complex model, as shown in Tables 5 and 6 for reciprocal and nonreciprocal translocations, respectively. Expanding the most restricted model to allow for different ratios of initial to asymptotic frequencies produced a significantly better fit ($P = 0.032$).

TABLE 4
Coefficient Estimates and Standard Errors of the "Best" Exponential Fit to Nonreciprocal Translocation Data from Day 8 through Day 365

Coefficient	Value	SE	*P* value
A_i (Asymptote)			
1 Gy	0.0×10^{-3}	1.1×10^{-3}	1.0
2 Gy	0.0×10^{-3}	2.2×10^{-3}	1.0
3 Gy	5.7×10^{-3}	1.1×10^{-3}	1.78×10^{-6}
4 Gy	8.3×10^{-3}	1.3×10^{-3}	8.66×10^{-9}
B_i (Initial)			
1 Gy	1.8×10^{-3}	1.2×10^{-3}	0.14
2 Gy	4.2×10^{-3}	2.2×10^{-3}	0.06
3 Gy	17.6×10^{-3}	5.5×10^{-3}	0.002
4 Gy	71.9×10^{-3}	22.2×10^{-3}	0.002
C_i (Decay)			
1 Gy	2.1	2.7	0.43
2 Gy	1.7	1.8	0.34
3 Gy	10.4	4.2	0.02
4 Gy	22.3	6.6	0.001
Dispersion			
θ	7.5	2.7	0.005

Notes. Model was of the form $A_i + B_i \exp(-C_i t)$, with all coefficients constrained to be non-negative. The errors in the outcome were assumed to contain extra-Poisson variation, the extent of which is estimated by θ. Only data from days 8 through 365 were used to estimate the coefficients. (See the Materials and Methods for details.)

Expanding that model to allow for different decay constants also produced a significantly better fit ($P = 0.048$). Therefore, the most complex model, $A_d + B_d \exp(-C_d t)$, produces the best fit for reciprocal and nonreciprocal translocations, even after adjusting for the increased number of parameters.

The asymptote estimates for reciprocal translocations are significantly different from each other and increase with dose, as expected (Table 3). The decay constants, on the other hand, are not significant at 2 Gy and below, indicating that we were unable to see a decrease in translocation frequency over time at those doses. However, the decay constants for 3 and 4 Gy were quite significantly different from zero, but not significantly different from each other (difference of approximately 6 with a standard error of 4.7). Figure 1 shows the data from 8 days onward, on which is superimposed the fitted background, decay curve, and their sum.

The decrease in translocations induced by the higher doses of radiation along with the increase in aberrations with age complicates the dose responsiveness, resulting in a nearly complete loss of dependence on dose 1 year after exposure. This is illustrated in Fig. 3, which shows a flattening of the dose–response curves over time.

Nonreciprocal translocations showed more rapid loss of translocations with time than reciprocal translocations (Table 4). As with reciprocal translocations, a likelihood ratio test (Table 6) indicated that the most complex model produced a significantly better fit than the least complex model, but the intermediate model was indistinguishable from the least complex model. Mice exposed to the highest doses (3 and 4 Gy) showed a significant decrease in nonreciprocal translocations in the first 3 months after exposure; beyond this time the frequency was stable and very close to baseline. As with reciprocal translocations, nonreciprocal translocations induced by 2 Gy and below did not show significant decay. Figure 2 shows the data from 8 days onward, on which is superimposed the fitted background, decay curve, and their sum.

Dicentric chromosomes decreased by almost 50% after 2 weeks, and almost none remained after 90 days (data not shown). No fits to these data were performed.

Clonal Expansion

We observed a number of clonal cells in peripheral blood lymphocytes (Fig. 4). Among mice exposed to 4 Gy, the mean frequencies of aberrant cell clones in peripheral blood lymphocytes ranged from 3 to 29% of the total number of metaphase cells scored with the highest frequency observed 1 year postexposure. A dose–response relationship for clones was evident until 21 months, when one unexposed animal exhibited a clone comprising >40% of the cells scored.

The presence of clones caused the mean frequency of aberrations at various times to be elevated, further complicating the dose response for translocations. To ameliorate this effect, we corrected the data for the presence of clones. It is obvious from comparing the data before and after correction that clonal expansion was responsible for a major fraction of the translocation frequencies (Fig. 5). We found that in mice exposed to 4 Gy, 32 to 70% of reciprocal translocations and 19 to 93% of nonreciprocal translocations were of clonal origin, with the highest value observed 1 year after exposure. One mouse exposed to 4 Gy exhibited a clone 1 year after exposure that contained two non-

TABLE 5
Likelihood Ratio Tests for the Three Models, Reciprocal Translocations

Model	Residual *df*	2 × log likelihood	Degrees of freedom	Likelihood ratio statistic	*P* value
1. $A_d\,[1 + B^{(-C\,t)}]$	122	3675.6	N/A[a]	N/A[a]	N/A[a]
2. $A_d + B_d^{(-C\,t)}$	119	3684.4	3	8.79	0.032
3. $A_d + B_d^{(-Cd\,t)}$	116	3692.3	3	7.91	0.048

[a] Not applicable.

TABLE 6
Likelihood Ratio Tests for the Three Models, Nonreciprocal Translocations

Model	Residual *df*	2 × log likelihood	Degrees of freedom	Likelihood ratio statistic	*P* value
1. $A_d\,[1 + B^{(-C\,t)}]$	120	1198.9	N/A[a]	N/A[a]	N/A[a]
2. $A_d + B_d^{(-C\,t)}$	117	1203.9	3	5.04	0.17
3. $A_d + B_d^{(-Cd\,t)}$	114	1212.6	3	8.72	0.033

[a] Not applicable.

reciprocal translocations and an insertion (data not shown). This clone constituted 257 (52%) of the 496 cells scored. Two subclasses of this clone were identified, one with another insertion and one with a reciprocal translocation in addition to the two aberrations in the original clone. The mouse bearing this clone appeared to be in good health with no evidence of malignancy.

While clonal expansion was not observed in every mouse, it was observed in a substantial number of animals, and at the higher doses the frequency of clones was high enough that correction was essential for obtaining a clear picture of the overall stability of translocations. Since correction eliminates the high degree of variation at the data points 90 days after exposure, a more accurate view of the persistence of reciprocal translocations can be seen, and an improved estimate of the percentage of the original translocations that are lost in those first 3 months can be determined. After correcting for clones, we found that 63% of reciprocal translocations and 79% of nonreciprocal translocations induced by 3 Gy and 68% of reciprocal translocations and 62% of nonreciprocal translocations induced by 4 Gy were lost over time. The remainder of these translocations appear to be completely persistent and would likely remain throughout the life span of the mice.

The dose–response calculations were much more precise after correction for clonal expansion. In fact, estimates for standard errors were too unstable numerically to calculate with uncorrected data. The improvement due to correction was quantified in two separate ways. First, the two overdispersion statistics, which measure two types of extra-Poisson variation (see the Materials and Methods), were calculated for both corrected and uncorrected data. For Poisson data, the two statistics are each distributed as a χ^2 with 1 degree of freedom. For reciprocal translocations, the overdispersion statistics for corrected data were 1.4 and 2.8 and were not significantly different from Poisson ($P = 0.24$ and 0.09, respectively). For uncorrected data, the statistics were 2771 and 685 ($P \cong 0$ in both cases). In addition, for both uncorrected and corrected data, observed means per 100 cell equivalents were calculated for the four nonzero doses across the seven times 90 days and later (i.e. the times when clonal expansion was corrected). Residual variance was calculated based on a model assuming independence of rows and columns. For the data on reciprocal and nonreciprocal translocations, the ratios of the sum of squared Pearson residuals before and after correction were 58 and 47, respectively, meaning that about 98% of the residual variation in the uncorrected data can be attributed to clones of abnormal cells. These results illustrate the importance of recognizing and correcting for the presence of extra-Poisson variation due to clonal aberrations at long times after exposure.

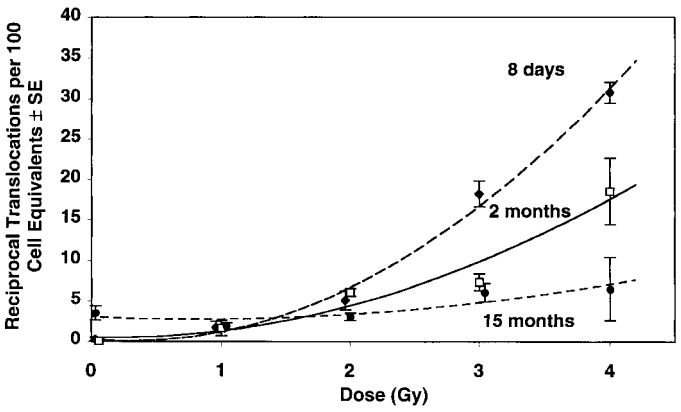

FIG. 3. Dose–response curves for reciprocal translocations at 8 days, 2 months and 15 months postirradiation. Note the almost complete lack of a dose response at 15 months due to the elevated translocation frequency in controls and the decline in translocation frequencies in the exposed animals. Some data points have been slightly offset on the horizontal axis for clarity.

DISCUSSION

Persistence of Translocations

Translocation frequencies have been expected by many investigators to remain stable over time, and several studies seem to have substantiated this hypothesis (*3, 23–26*). However, in studies of the atomic bomb survivors (*3, 23*), no initial cytogenetic measurements were made shortly after exposure. Therefore, an initial decline would have been missed. The study of Lucas *et al.* (*25*) and the follow-up study by Lloyd *et al.* (*26*) involved a very low dose (0.4 Gy) of radiation to a worker accidentally exposed to tritiated water. This study showed that the frequency of translocations measured 11 years after the accident was not significantly different from the frequency of dicentrics measured within a few weeks of exposure. In contrast to these findings, a study of Goiania accident victims, which involved higher doses, showed that translocation frequencies had decreased 1 year after exposure (*27*).

We previously reported (*16*) that the decrease in trans-

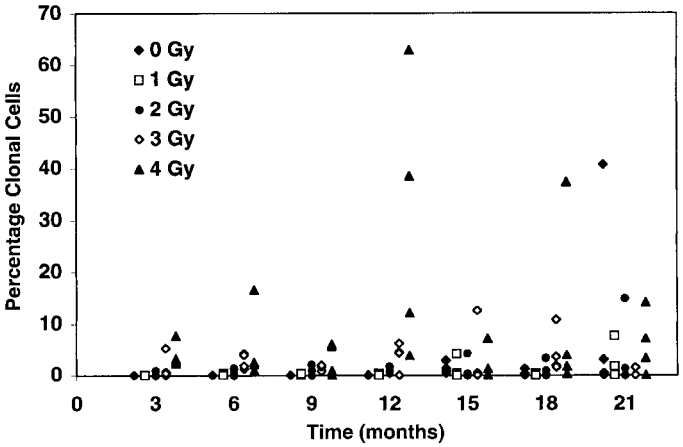

FIG. 4. Percentage of peripheral blood cells in each animal with chromosome aberrations that are clonal. Each symbol represents an individual mouse at the indicated dose and time. Data are offset on the horizontal axis by dose group for clarity.

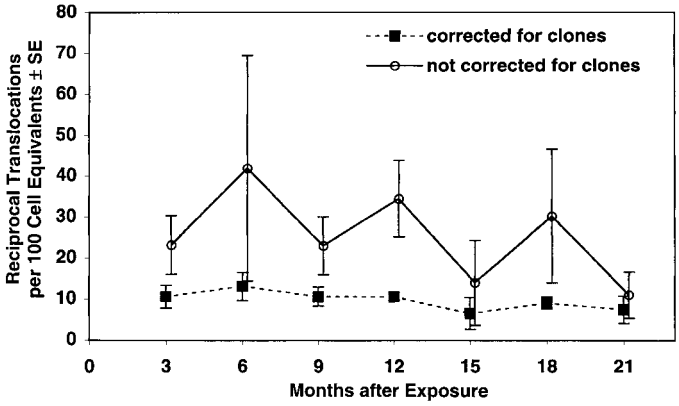

FIG. 5. Comparison of reciprocal translocation frequencies in mice exposed to 4 Gy ^{137}Cs γ rays before and after correction for clonal expansion. Vertical bars represent the standard errors. The uncorrected data points are offset slightly on the horizontal axis for clarity.

location frequency in the peripheral blood of acutely exposed mice seemed to correlate with the elimination of heavily damaged cells that may have carried unstable events. Similar to our study, Fernandez *et al.* (*28*) and Tucker *et al.* (*17*) observed decreases in translocations induced *in vitro* in human and rat peripheral blood lymphocytes, respectively. However, each group concluded that this decrease could be due to cells carrying both stable and unstable events only if cells containing translocations were somehow more likely also to contain one or more unstable events. Fernandez *et al.* (*28*) found no such correlation, although they speculated that high-LET radiation or nonuniform exposure to low-LET radiation could give this result. In our study, great care was taken to ensure uniform radiation exposure. Matsumoto *et al.* (*9*) showed in human peripheral blood lymphocytes acutely exposed to ^{137}Cs γ rays *in vitro* that first-division cells carrying translocations are more likely to have dicentrics than cells without translocations. A significant reduction of translocations was observed out to 7 days after exposure at all doses. Their data also suggest that the loss of cells containing dicentrics might be partially responsible for the decline in translocations. Guerrero-Carbajal *et al.* (*29*) explained that theoretically the distributions of translocations and dicentrics are Poisson and independent in whole-body irradiation, but that with partial-body irradiation, the distributions are linked since they are confined to the fraction of irradiated cells. They argued that there would logically be a decrease in translocations in partial-body irradiation due to the presence of dicentrics in the same cells, but due to the independent distributions, whole-body irradiation should not give the same result. This was demonstrated experimentally with simulated whole- and partial-body irradiation *in vitro*; however, relatively few cells were scored. We have demonstrated that *in vivo* whole-body irradiation does result in an initial decline in stable aberrations; however, this may not be due to the presence of unstable aberrations in the same cells. Hande and Natarajan (*30*) recently reported a similar decline in the frequency of translocations in splenocytes in the first 112 days after whole-body exposure to X radiation. They showed that the decline was still apparent when the analysis was performed on cells with only one aberration, suggesting that another mechanism besides the presence of unstable aberrations was responsible.

Diminished persistence of cells with translocations might be due to imbalances at the molecular level. Deletions of up to 8 kb can result during the repair of double-strand breaks (*31*), and chromosome painting does not offer the resolution to detect this deleted material. Kodama *et al.* (*32*) estimated the minimum size for detection of translocated segments by chromosome painting to be 11.1 Mb. It is also expected that some of the rearrangements which appear to be translocations are actually more complex aberrations in which blocks of chromatin are brought together in abnormal combinations that make the cells containing them nonviable. In addition, some radiation-induced damage affects single genes that cannot be observed at the chromosomal level. After significant amounts of cell death, the restoration of the lymphocyte population from undamaged stem cells will result in the dilution of abnormal cells (*24*). Our observations of clonal expansion show that damaged stem cells may also be repopulating the peripheral blood, causing an increase in aberration frequencies over time.

Chromosome aberration frequencies have previously been shown to increase with age in ''unexposed'' human populations (*6, 33–39*). Similar findings were recently reported in mice (*22*), and these results were based in part on the unexposed animals in the experiment described here. Since clastogens and mutagens are part of our everyday environment, including background radiation and chemicals in food and drinking water and air, there really are no unexposed individuals. Furthermore, humans are known to respond differently to certain chemicals due to genetic differences. However, the experiment described here was designed to minimize the effects of differences in genetic and

environmental factors. All of the animals were inbred C57BL/6 females, housed in the same facility, fed the same pelleted food, and given the same drinking water, so as to be as uniform as possible. The increase in translocation frequencies with age thus suggests the existence of inherent biological processes, and this has been discussed in detail elsewhere (*22*).

Clonal Expansion

There is a substantial amount of evidence for the presence of clones bearing radiation-induced chromosome rearrangements (*40–49*), yet some have concluded that translocation frequencies and subsequent dose estimates should not be significantly influenced by the presence of these clones (*3, 50*). Salassidis *et al.* (*45*) observed a clone which comprised 5.5–9% of cells analyzed in one patient and which contributed 16.5–23.5% of the total translocation frequency. They concluded that correction for clonal expansion is mandatory if clonal contribution makes the translocation frequency >3 standard deviations higher than the corrected frequency. Numerous subjects with clones of abnormal cells have been observed in Chernobyl cleanup workers (*49*) as well as in healthy, unexposed subjects (*38, 46*). In general, clones appear to be more prevalent in older subjects, they are not always obvious to the casual observer, and their frequency can vary tremendously (*48*). The results of the present study support the conclusion that correction for clonality is necessary in biodosimetry studies.

Clones in the peripheral blood could arise from expansion of a mature lymphocyte as a result of immunological stimulation, or by differentiation of stem cells bearing stable aberrations (*44*). In the present study, it is impossible to speculate which, if either, of these phenomena occurred or if the high frequency of clones is indicative of a premalignant process. Kusunoki *et al.* (*44*) studied clonal expansion in one A-bomb survivor. One aberrant cell clone comprised 3–8% of the peripheral blood lymphocytes. Because the frequency of clonal cells remained constant for 10 years, they concluded that positive selection due to a selective growth advantage of a cell bearing a particular translocation was unlikely. Furthermore, they suggest that a single stem cell of an adult is able to generate lymphocyte progenies that amount to several percent of the total population. In our work, one clone was observed to account for as many as 52% of the peripheral blood cells 1 year after exposure, suggesting that mice may have substantially fewer stem cells than humans.

We observed considerable variability in the appearance of clones. Perhaps this is due to the fraction of lymphocytes that have much longer life spans. Theoretically, in the absence of a selective growth advantage, we should not see a change in translocation frequencies due to the normal division/repopulation of stem cells. This is assuming that division is random and occurs with equal frequency in all stem cells. However, if the kinetics of all stem cells is not equal (i.e., some are active while others are inactive), then increases or decreases in translocation frequencies are entirely possible. Since we were able to sample each mouse only once, we cannot determine the extent or the magnitude of changes in the frequencies of clones of abnormal cells over time.

Equality of Translocation and Dicentric Frequencies

As we reported previously (*16*), translocations and dicentrics were induced at equal frequencies in peripheral blood lymphocytes. This is consistent with theoretical expectations and has been demonstrated experimentally (*12, 14, 51, 52*). There remains much debate, however, since many studies have reported conflicting results (*4, 5, 7, 10, 53, 54*). Most of the studies reporting equality were performed in mice. Hande *et al.* (*14*) theorized that the difference between the induction of equal frequencies of translocations and dicentrics in humans and mice is due to the fact that humans possess both metacentric and acrocentric chromosomes, while only acrocentrics are found in mice. Translocations, unlike dicentrics, are not limited by the number of centromeres in a cell, so the presence of more chromosome arms increases the probability of formation of translocations. This theory is supported in a study by Dominguez *et al.* (*55*), who showed that X rays induced more translocations than dicentrics in Chinese hamster cells, which possess metacentric chromosomes. Lucas *et al.* (*56*) argued that equality of the frequencies of translocations and dicentrics exists, but only rearrangements where there appears to be a single complete reciprocal exchange should be included in the comparison.

Our results provide evidence for a common rate ratio for translocations and dicentrics at day 1, but not at day 8. The lack of a common rate ratio at 8 days may be hypothesized to be due to a loss of dicentrics that is dependent on dose as well as time since exposure. At low doses there would be little effect of the radiation on replenishment of the peripheral lymphocyte population by cell cycling because there is little cell killing and the level of damage is low enough to preclude large delays by the cell cycle control checkpoint mechanisms. At high doses many cells will be killed and surviving cells may experience long delays; thus the disappearance rate for dicentrics may be slower, since dicentrics are lost only when cells go through mitosis. At intermediate doses, it is possible that replenishment of the lymphocyte population through cell division is sufficiently fast to allow for a marked loss of dicentrics 8 days after *in vivo* exposure.

Summary

We have provided quantitative information over the lifetime of a rodent on the stability of reciprocal and nonreciprocal translocations induced *in vivo* by ionizing radiation. The loss of nonpersistent translocations and the gain of translocations either by clonal expansion or by the aging

process can lead to under- or overestimates of radiation exposures. Age and clonal expansion have been shown to be confounding factors which may have ramifications for biological dosimetry in humans. By recognizing the loss of translocations over time and the important role of clonal expansion and aging, retrospective biological dosimetry in humans may be substantially improved.

APPENDIX

Curve-Fitting Methods and Overdispersion

Fitting Exponential Curves

A nested series of three exponential decay models was fitted to a subset of the data for each outcome. Only data for dose >0 and time between 8 and 365 days were used in the exponential fits. Dose = 0 was omitted because background was estimated separately using the data for dose = 0, with the resulting estimated background used as constants in subsequent exponential fits. The data beyond 1 year were omitted because the background effect begins to dominate the fit after this time, interfering with the accurate determination of the asymptote. The decay curves in Figs. 1 and 2 represent extrapolations beyond 1 year based on the data up to 1 year after exposure.

Each set of observations for a given dose d and time t was assumed to be a random sample from either a Poisson distribution with mean $N_{dtk}Y_d(t)$ or a negative binomial distribution with mean $N_{dtk}Y_d(t)$ and unknown shape parameter θ, where N_{dt} is the number of cells scored for that dose–time combination for mouse k. [For a description of negative binomial models, see ref. (*21*)]. The specific distribution used depended on whether or not a significant amount of overdispersion was observed. The data for reciprocal translocations were not significantly overdispersed between days 8 and 365, so Poisson errors were used. On the other hand, the nonreciprocal translocations were significantly overdispersed, so negative binomial errors were used to fit the data for nonreciprocal translocations.

For purposes of model selection only, means were taken as

$$Y_d(t) = b\ (t) + A_d\ [1 + B_d \exp(-C_d\ t)],$$

where $Y_d(t)$ is the average outcome for dose d (in grays) and time t (in years). In this model, the previously estimated background at time t is represented by $b(t)$, the average initial value for dose d is $A_d\ (1 + B_d)$, and the asymptote is A_d. Hence the ratio of initial value to asymptote is $1 + B_d$ irrespective of the value of the asymptote. The decay constant is C_d. Two nested sub-models were created. The first assumed that the decay constant was the same across all doses (constant C), and the second assumed that both the decay constant and ratio of initial to asymptotic average values were the same across all doses (constant B and C). Note that for reporting purposes (Tables 3 and 4), the model equation used is the standard one:

$$Y_d(t) = b\ (t) + A_d + B_d \exp(-C_d\ t).$$

The fits were performed by non-negatively constrained maximum likelihood, using the nlminb routine in S-PLUS (*57*). When possible, standard deviations were estimated by inverting a finite-difference approximation to the Hessian using the vcov.nlminb routine.

Accounting for Overdispersion

We accounted for detected overdispersion by fitting negative binomial models to data where overdispersion was clearly present. Negative binomial fits produce the same estimates as Poisson models, but produce more realistic standard errors along with an estimate of the amount of overdispersion. For negative binomial random variables, the mean variance relationship is given by

$$V(\mu) = \mu\ (1+\mu/\theta),$$

where θ is estimated by maximum likelihood. Smaller values of θ correspond to overdispersion that increases more like the square of the mean, while an infinite θ corresponds to Poisson variation.

ACKNOWLEDGMENTS

This work was performed in part under the auspices of the U.S. DOE by the Lawrence Livermore National Laboratory under contract No. W-7405-ENG-48. This paper is published with the approval of the Director of the West Virginia Agriculture and Forestry Experiment Station as Scientific Paper Number 2725.

Received: May 10, 1999; accepted: September 15, 1999

REFERENCES

1. D. O. Stram, R. Sposto, D. Preston, S. Abrahamson, T. Honda and A. A. Awa, Stable chromosome aberrations among A-bomb survivors: An update. *Radiat. Res.* **136**, 29–36 (1993).
2. D. H. Moore II, J. D. Tucker, I. M. Jones, R. G. Langlois, P. Pleshanov, I. Vorobtsova and R. Jensen, A study of the effects of exposure on cleanup workers at the Chernobyl nuclear reactor accident using multiple end points. *Radiat. Res.* **148**, 463–475 (1997).
3. J. N. Lucas, A. Awa, T. Straume, M. Poggensee, Y. Kodama, M. Nakano, K. Ohtaki, H. U. Weier, D. Pinkel and L. G. Littlefield, Rapid translocation frequency analysis in humans decades after exposure to ionizing radiation. *Int. J. Radiat. Biol.* **62**, 53–63 (1992).
4. A. T. Natarajan, R. C. Vyas, F. Darroudi and S. Vermeulen, Frequencies of X-ray-induced chromosome translocations in human peripheral lymphocytes as detected by in situ hybridization using chromosome-specific DNA libraries. *Int. J. Radiat. Biol.* **61**, 199–203 (1992).
5. M. Bauchinger, E. Schmid, H. Zitzelsberger, H. Braselmann and U. Nahrstedt, Radiation-induced chromosome aberrations analysed by two-colour fluorescence *in situ* hybridization with composite whole chromosome-specific DNA probes and a pancentromeric DNA probe. *Int. J. Radiat. Biol.* **64**, 179–184 (1993).
6. M. J. Ramsey, D. H. Moore II, J. F. Briner, D. A. Lee, L. A. Olsen, J. R. Senft and J. D. Tucker, The effects of age and lifestyle factors on the accumulation of cytogenetic damage as measured by chromosome painting. *Mutat. Res.* **338**, 95–106 (1995).
7. J. D. Tucker, M. J. Ramsey, D. A. Lee and J. L. Minkler, Validation of chromosome painting as a biodosimeter in human peripheral blood lymphocytes following acute exposure to ionizing radiation *in vitro*. *Int. J. Radiat. Biol.* **64**, 27–37 (1993).
8. J. D. Tucker, W. F. Morgan, A. A. Awa, M. Bauchinger, D. Blakey, M. N. Cornforth, L. G. Littlefield, A. T. Natarajan and C. Shasserre, A proposed system for scoring structural aberrations detected by chromosome painting. *Cytogenet. Cell Genet.* **68**, 211–221 (1995).
9. K. Matsumoto, M. J. Ramsey, D. O. Nelson and J. D. Tucker, Persistence of radiation-induced translocations in human peripheral blood determined by chromosome painting. *Radiat. Res.* **149**, 602–613 (1998).
10. J. W. Breneman, M. J. Ramsey, D. A. Lee, G. G. Eveleth, J. L. Minkler and J. D. Tucker, The development of chromosome-specific composite DNA probes for the mouse and their application to chromosome painting. *Chromosoma* **102**, 591–598 (1993).
11. J. M. Breneman, R. R. Swiger, M. J. Ramsey, J. L. Minkler, G. G. Eveleth, R. Langlois and J. D. Tucker, The development of painting probes for dual color and multiple chromosome analysis in the mouse. *Cytogenet. Cell Genet.* **68**, 197–202 (1995).
12. J. J. W. A. Boei, A. S. Balajee, P. De Boer, W. Rens, A. Aten, L. H. F. Mullenders and A. T. Natarajan, Construction of mouse chromosome-specific DNA libraries and their use for the detection of X-ray-induced aberrations. *Int. J. Radiat. Biol.* **65**, 583–590 (1994).
13. A. E. Director, J. Nath, M. J. Ramsey, R. R. Swiger and J. D. Tucker,

Cytogenetic analysis of mice chronically fed the food mutagen 2-amino-1-methyl-6-phenylimidazo[4,5b] pyridine (PhIP). *Mutat. Res.* **359**, 53–61 (1996).

14. M. P. Hande, J. J. Boei, F. Granath and A. T. Natarajan, Induction and persistence of cytogenetic damage in mouse splenocytes following whole-body X-irradiation analysed by fluorescence *in situ* hybridization. I. Dicentrics and translocations. *Int. J. Radiat. Biol.* **69**, 437–446 (1996).

15. P. Rabbitts, H. Impey, A. Heppell-Parton, C. Langford, C. Tease, N. Lowe, D. Bailey, M. Ferguson-Smith and N. Carter, Chromosome specific paints from a high resolution flow karyotype of the mouse. *Nat. Genet.* **9**, 369–375 (1995).

16. M. D. Spruill, M. J. Ramsey, R. R. Swiger, J. Nath and J. D. Tucker, The persistence of aberrations in mice induced by gamma radiation as measured by chromosome painting. *Mutat. Res.* **356**, 135–145 (1996).

17. J. D. Tucker, J. W. Breneman, J. F. Briner, G. G. Eveleth, R. G. Langlois and D. H. Moore II, The persistence of radiation-induced translocations in rat peripheral blood determined by chromosome painting. *Environ. Mol. Mutagen.* **30**, 264–272 (1997).

18. H. Evans, Chromosome aberrations induced by ionizing radiations. *Int. Rev. Cytol.* **13**, 221–320 (1962).

19. C. Disteche, A. Carrano, L. Ashworth, K. Burkhart-Schultz and S. Latt, Flow sorting of the mouse Cattanach X chromosome, T(X:7) 1 Ct, in an active or inactive state. *Cytogenet. Cell Genet.* **29**, 189–197 (1981).

20. A. Agresti, *Categorical Data Analysis*. Wiley, New York, 1990.

21. W. N. Venables and B. D. Ripley, *Modern Applied Statistics with S-PLUS*, 2nd ed. Springer-Verlag, New York, 1997.

22. J. D. Tucker, M. D. Spruill, M. J. Ramsey, A. D. Director and J. Nath, Frequency of spontaneous chromosome aberrations in mice: Effects of age. *Mutat. Res.* **425**, 135–141 (1999).

23. A. Awa, T. Sofuni, T. Honda, M. Itoh, S. Neriishi and M. Otake, Relationship between the radiation dose and chromosome aberrations in atomic bomb survivors of Hiroshima and Nagasaki. *J. Radiat. Res.* **19**, 126–140 (1978).

24. K. E. Buckton, G. E. Hamilton, L. Paton and A. O. Langlands, Chromosome aberrations in irradiated ankylosing spondylitis patients. In *Mutagen-Induced Chromosome Damage in Man* (H. J. Evans and D. C. Lloyd, Eds.), pp. 142–150. University Press, Edinburgh, 1978.

25. J. N. Lucas, M. Poggensee and T. Straume, The persistence of chromosome translocations in a radiation worker accidentally exposed to tritium. *Cytogenet. Cell Genet.* **60**, 255–256 (1992).

26. D. C. Lloyd, J. E. Moquet, S. Oram, A. A. Edwards and J. N. Lucas, Accidental intake of tritiated water: A cytogenetic follow-up case on translocation stability and dose reconstruction. *Int. J. Radiat. Biol.* **73**, 543–547 (1998).

27. T. Straume, R. G. Langlois, J. Lucas, R. H. Jensen, W. L. Bigbee, A. G. Ramalho and C. E. Brandao-Mello, Novel biodosimetry methods applied to victims of the Goiania accident. *Health Phys.* **60**, 71–76 (1991).

28. J. L. Fernandez, A. Campos, V. Goyanes, C. Losada, C. Veiras and A. A. Edwards, X-ray biological dosimetry performed by selective painting of human chromosomes 1 and 2. *Int. J. Radiat. Biol.* **67**, 295–302 (1995).

29. Y. C. Guerrero-Carbajal, J. E. Moquet, A. A. Edwards and D. C. Lloyd, The persistence of FISH translocations for retrospective biological dosimetry after simulated whole or partial body irradiation. *Radiat. Prot. Dosim.* **76**, 159–168 (1998).

30. M. P. Hande and A. T. Natarajan, Induction and persistence of cytogenetic damage in mouse splenocytes following whole-body X-irradiation analysed by fluorescence *in situ* hybridization. IV. Dose response. *Int. J. Radiat. Biol.* **74**, 441–448 (1998).

31. L. H. Lutze, J. E. Cleaver, W. F. Morgan and R. A. Winegar, Mechanisms involved in rejoining DNA double-strand breaks induced by ionizing radiation and restriction enzymes. *Mutat. Res.* **299**, 225–232 (1993).

32. Y. Kodama, M. Nakano, K. Ohtaki, R. Delongchamp, A. Awa and N. Nakamura, Estimation of minimal size of translocated chromosome segments detectable by fluorescence *in situ* hybridization. *Int. J. Radiat Biol.* **71**, 35–39 (1997).

33. R. T. Dutkowski, R. Lesh, L. Staiano-Coico, H. Thaler, G. J. Darlington and M. E. Weksler, Increased chromosomal instability in lymphocytes from elderly humans. *Mutat. Res.* **149**, 505–512 (1985).

34. G. A. Harris, S. A. Holmes, W. A. Sabovlijev, M. Cramp, S. Hedges, J. M. Hornsey and G. C. Bennet, Sensitivity to X-irradiation of peripheral lymphocytes from aging donors. *Int. J. Radiat. Biol.* **50**, 685–694. (1986).

35. M. Prieur, W. Al Achkar, A. Aurias, J. Couturier, A.M. Dutrillaux, B. Dutrillaux, A. Flury-Herard, M. Gerbault-Seureau, F. Hoffschir and E. Viegas-Pequignot, Acquired chromosome rearrangements in human lymphocytes: Effect of aging. *Hum. Genet.* **79**, 147–150 (1988).

36. B. B. Ganguly, Cell division, chromosomal damage and micronucleus formation in peripheral lymphocytes of healthy donors: related to donor's age. *Mutat. Res.* **295**, 135–148 (1993).

37. J. Pincheira, C. Gallo, M. Bravo, M. H. Navarrete and J. F. Lopez-Saez, G_2 repair and aging: Influence of donor age on chromosomal aberrations in human lymphocytes. *Mutat. Res.* **295**, 55–62 (1993).

38. J. D. Tucker, D. A. Lee, M. J. Ramsey, J. Briner, L. Olsen and D. H. Moore II, On the frequency of chromosome exchanges in a control population measured by chromosome painting. *Mutat. Res.* **313**, 193–202 (1994).

39. H. Weirich-Schwaiger, H. G. Weirich, B. Gruber, M. Schweiger and M. Hirsh-Kauffmann, Correlation between senescence and DNA repair in cells from young and old individuals and in premature aging syndromes. *Mutat. Res.* **316**, 37–48 (1994).

40. A. A. Awa, Cytogenetic and oncogenic effects of the ionizing radiations of the atomic bombs. In *Chromosomes and Cancer* (J. German, Ed.), pp. 637–674. Wiley, New York, 1974.

41. J. R. K. Savage and T. R. L. Bigger, Aberration distribution and chromosomally marked clones in X-irradiated cells. In *Mutagen-Induced Chromosome Damage in Man* (H. J. Evans and D. C. Lloyd, Eds.), pp. 155–169. University Press, Edinburgh, 1978.

42. M. Mouthuy and B. Dutrillaux, Cytogenetic study of skin fibroblasts in a case of accidental acute irradiation. *Mutat. Res.* **95**, 19–30 (1982).

43. L. G. Littlefield, R. A. Kleinerman, A. M. Sayer, R. Tarone and J. D. Boice, Jr., Chromosome aberrations in lymphocytes—biomonitors of radiation exposure. *Prog. Clin. Biol. Res.* **372**, 387–397 (1991).

44. Y. Kusunoki, Y. Kodama, Y. Hirai, S. Kyoizumi, N. Nakamura and M. Akiyama, Cytogenetic and immunologic identification of clonal expansion of stem cells into T and B lymphocytes in one atomic-bomb survivor. *Blood* **86**, 2106–2112 (1995).

45. K. Salassidis, V. Georgiadou-Schumacher, H. Braselmann, P. Muller, R. U. Peter and M. Bauchinger, Chromosome painting in highly irradiated Chernobyl victims: A follow-up study to evaluate the stability of symmetrical translocations and the influence of clonal aberrations for retrospective dose estimation. *Int. J. Radiat. Biol.* **68**, 257–262 (1995).

46. K. L. Johnson, J. D. Tucker and J. Nath, Frequency, distribution and clonality of chromosome damage in human lymphocytes by multicolor FISH. *Mutagenesis* **13**, 217–227 (1998).

47. K. L. Johnson, J. W. Breneman III, J. Kunich, K. Matsumoto, M. J. Ramsey, K. J. Sorensen and J. D. Tucker, Fluorescence *in situ* hybridization of human and rodent DNA probes to determine the chromosomal contents of tissues, cell lines, and tumors. In *Cell Biology: A Laboratory Handbook*, 2nd ed., Vol. 3, pp. 444–452. Academic Press, San Diego, 1997.

48. K. L. Johnson, D. J. Brenner, J. Nath, J. D. Tucker and C. R. Geard, Radiation-induced breakpoints in human chromosomes: Random or non-random? *Int. J. Radiat. Biol.* **75**, 131–141 (1999).

49. K. L. Johnson, J. Nath, J. Pluth and J. D. Tucker, The distribution of chromosome damage, non-reciprocal translocations and clonal aberrations in lymphocytes from Chernobyl clean-up workers. *Mutat. Res.* **439**, 77–85 (1999).

50. A. Maes, A. Hilali, E. D. Léonard, A. Léonard and L. Verscheve,

Stable chromosome aberrations 25 years after severe accidental radiation exposure. *Radiat. Environ. Biophys.* **32**, 319–324 (1993).

51. J. A. Heddle, Randomness in the formation of radiation-induced chromosome aberrations. *Genetics* **52**, 1320–1334 (1965).

52. K. Buckton, Identification with G and R banding of the position of breakage points induced in human chromosomes by *in vitro* X-irradiation. *Int. J. Radiat. Biol.* **29**, 475–488 (1976).

53. E. Schmid, H. Zitzelsberger, H. Braselmann, J. W. Gray and M. Bauchinger, Radiation-induced chromosome aberrations analysed by fluorescence *in situ* hybridization with a triple combination of composite whole chromosome-specific DNA probes. *Int. J. Radiat. Biol.* **62**, 673–678 (1992).

54. J. D. Tucker, D. A. Lee and D. H. Moore II, Validation of chromosome painting II: A detailed analysis of aberrations following high doses of ionizing radiation *in vitro*. *Int. J. Radiat. Biol.* **67**, 19–28 (1995).

55. I. Dominguez, W. A. Boei, A. Balajee and A. Natarajan, Analysis of radiation-induced chromosome aberrations in Chinese hamster cells by FISH using chromosome-specific DNA libraries. *Int. J. Radiat. Biol.* **70**, 199–208 (1996).

56. J. Lucas, A. Chen and R. Sachs, Theoretical predictions on the equality of radiation-produced dicentrics and translocations detected by chromosome painting. *Int. J. Radiat. Biol.* **69**, 145–153 (1996).

57. Mathsoft S-PLUS User's Guide, Data Analysis Products Division, Seattle, WA, 1997.